Safety-Critical Adaptive Cruise Control via Control Lyapunov and Control Barrier Function - Quadratic Program

Prateek Chauhan[a] **and Tejas M. Bhade**[b]

[a]*MS Mech, BE Mech*
[b]*MS Robotics, BE Mech*

Dr. Chaozhe He, Ph.D.

Abstract—This report presents the design and simulation of an Adaptive Cruise Control (ACC) system for a heavy-duty Class-8 truck. A nominal Connected Cruise Control (CCC) law is augmented by a Control-Lyapunov-Function / Control-Barrier-Function Quadratic Program (CLF–CBF–QP) to guarantee safety (minimum headway) while retaining performance. Three lead-vehicle profiles—including a severe braking scenario—are evaluated. Results confirm forward-collision avoidance, smooth speed tracking, and real-time feasibility.

Keywords— *ACC, CLF, CBF, QP*

1. Introduction

Adaptive Cruise Control (ACC) lets a vehicle follow a lead car by automatically matching its speed and keeping a comfortable gap. In this highway-driving study the **ego vehicle is a Class 8 truck**, and the **lead vehicle is a typical passenger car**. The truck's greater mass and longer stopping distance make safety harder to guarantee when the lighter lead car brakes hard or accelerates suddenly.

To address this challenge, we build a safety-critical controller that blends two control ideas:

- **Control Lyapunov Functions (CLFs)** guide the truck toward its desired speed.
- **Control Barrier Functions (CBFs)** impose a minimum headway so the truck never leaves a collision-free safety set.

Both objectives are enforced at every time step by solving a single **Quadratic Program (QP)** that prioritises safety first and speed-tracking second.

A **nominal reference acceleration** $u_{\mathbf{ref}}$—inspired by Cooperative Connected Cruise Control (CCC) formulas—is computed locally from the simulated relative distance and speed. No real V2X link or physical sensors are used; instead, ground-truth states from the MATLAB simulation (optionally corrupted with Gaussian noise) act as measurements. The QP tries to follow u_{ref} whenever it does not conflict with the CBF constraint.

Key contributions

1. **Unified CLF-CBF-QP formulation**: a single optimisation that guarantees safety while preserving ride comfort for a heavy truck.
2. **V2X-style reference tracking**: a CCC-inspired u_{ref} that needs only simulated relative states.
3. **Comprehensive evaluation**: MATLAB simulations with four lead-car profiles (steady cruise, sudden brake, speed ramp, and noisy cruise) show the controller maintains headway, respects truck acceleration limits, and remains feasible even under extreme scenarios—outperforming a baseline ACC that lacks safety constraints.

2. Ego-Vehicle Longitudinal Dynamics

2.1. Concept

The Class 8 truck is represented by Longitudinal Bicycle Model. The longitudinal state vector is (D, v, v_L), where D is the bumper-to-bumper gap, v the truck speed, and v_L the lead-car speed.

The speed dynamics include two resistive forces

$$F_{\mathrm{drag}} = \frac{1}{2}\,\rho\, C_d\, A\, v^2, \qquad F_{\mathrm{roll}} = \mu_r\, m\, g\,.$$

Drag grows with v^2, while rolling resistance is nearly constant and switches sign with the travel direction. These forces appear in the open-loop vector field $f(x)$ used in the CLF and CBF calculations.

The ACC model is

$$\boxed{\begin{aligned} \dot{D} &= v_L - v, \\ \dot{v} &= u \;-\; \frac{F_{\mathrm{drag}} + F_{\mathrm{roll}}}{m}, \\ \dot{v}_L &= a_L, \end{aligned}} \tag{1}$$

where u is the control acceleration returned by the CLF-CBF-QP and a_L is the prescribed lead-car acceleration from the selected profile. This three-state system underpins the Lyapunov function, barrier function, and quadratic-program formulations that follow.

Table 1. Parameters for the ACC simulation.

Parameter	Value
Mass, m	18 000 kg
Drag coefficient, C_d	0.60
Frontal area, A	10 m^2
Rolling-resistance coefficient, μ_r	0.010
Gravity, g	9.81 m s^{-2}
Simulation time step, T_s	0.001 s

3. Control–Lyapunov Function (CLF) and Stability

3.1. Concept

A Control–Lyapunov Function is a positive-definite scalar map $V : \mathbb{R}^n \to \mathbb{R}_{\geq 0}$ satisfying (i) $V(x) = 0$ only at the desired equilibrium and (ii) $\dot{V} < 0$ is achievable for all $x \neq 0$. Maintaining $\dot{V} \leq -\gamma(V)$ for some class-$\mathcal{K}$ function γ guarantees asymptotic stability.

3.2. Sliding variables and CLF candidate

$$e = D - \tau_{\mathrm{clf}}\, v, \qquad z = (v_L - v) + \lambda\, e, \tag{2}$$

- **Gap** D — bumper-to-bumper distance between the lead car and the ego truck (m).
- **Desired time–gap spacing** $\tau_{\mathbf{clf}}\, v$ — the gap that exactly satisfies the chosen time-headway rule at speed v.
- **Headway constant** $\tau_{\mathbf{clf}}$ — Lyapunov design parameter (here 1.8 s), deliberately smaller than the safety headway $\tau_C BF$ so the CLF can tighten the gap without violating the CBF.
- **Spacing error**
$$e = D - \tau_{\mathrm{clf}}\, v,$$
- **Composite variable**
$$z = (v_L - v) + \lambda\, e,$$
combining the relative speed $v_L - v$ with the spacing error.
- **Damping factor** λ — a positive gain (s^{-1}) that weights the gap term in z.

With these definitions, the control-Lyapunov candidate is

$$V(x) = \tfrac{1}{2}\, z^2,$$

a positive definite function - measure of the squared distance to the manifold $z = 0 \Leftrightarrow (D, v) = (\tau_{\text{clf}} v, v_L)$.

3.3. Gradient and Lie derivatives

$$\nabla_x V = z\big[\lambda,\ -(1+\lambda\tau_{\text{clf}}),\ 1\big], \tag{3}$$

$$f(x) = \begin{bmatrix} v_L - v \\ -\dfrac{F_{\text{drag}}(v) + F_{\text{roll}}(v)}{m} \\ a_L \end{bmatrix},\ g(x) = \begin{bmatrix} 0 \\ 1 \\ 0 \end{bmatrix}, \tag{4}$$

$$\boxed{\begin{aligned} L_f V &= z\Big[\lambda(v_L - v) - \big(1+\lambda\tau_{\text{clf}}\big)\frac{F_{\text{drag}} + F_{\text{roll}}}{m} + a_L\Big], \\ L_g V &= z\big(-1 - \lambda\tau_{\text{clf}}\big). \end{aligned}} \tag{5}$$

3.4. Class-$\mathcal{K}$ function and relaxed inequality

Choose the linear class-$\mathcal{K}$ function

$$\gamma(V) = \varepsilon V, \qquad \varepsilon > 0.$$

Introduce slack $\delta \geq 0$:

$$L_f V + L_g V\, u \ \leq\ -\varepsilon V + \delta, \qquad \delta \geq 0. \tag{6}$$

The *infimum* $\inf_{u\in\mathbb{R}}\big[L_f V + L_g V\, u\big]$ is the steepest decrease attainable at state x.

3.5. Admissible set

$$K_{\text{clf}}(x) = \big\{(u,\delta) \mid (6),\ \delta \geq 0\big\};\ u \in \mathcal{U} := [\,u_{\min},\, u_{\max}\,]$$

3.6. Stability via LaSalle

With $(u,\delta) \in K_{\text{clf}}(x)$ and a large slack weight p,

$$\dot V \leq -\varepsilon V + \delta \leq -(\varepsilon - p^{-1})V \ \Rightarrow\ V(t) \leq V(0)\, e^{-(\varepsilon - p^{-1})t}.$$

LaSalle's principle yields convergence to $\{V = 0\} \equiv \{z = 0\}$, i.e. the desired headway manifold.

Table 2. CLF design parameters.

Parameter	Symbol	Value
Time headway	τ_{clf}	1.8 s
Damping	λ	0.5 s^{-1}
Decay rate	ε	0.10
Slack weight	p	100

4. Control–Barrier Function (CBF) and Safety

4.1. Concept

For the affine system $\dot x = f(x) + g(x)u$ a continuously differentiable map $h : \mathbb{R}^n \to \mathbb{R}$ is a *relative–degree–one control–barrier function* (CBF) if there exists an *extended class–$\mathcal{K}^\infty$* function α such that

$$\sup_{u\in\mathbb{R}^m}\big[L_f h(x) + L_g h(x)\, u\big] \ \geq\ -\alpha\big(h(x)\big), \qquad \forall x. \tag{7}$$

Any feedback input $u(x)$ that satisfies

$$L_f h(x) + L_g h(x)\, u(x) + \alpha\big(h(x)\big) \ \geq\ 0 \tag{8}$$

renders the *0-super-level set* $\mathcal{C} = \{x : h(x) \geq 0\}$ forward-invariant.

4.2. Barrier definition for longitudinal safety

$$\boxed{h(x) = D - \big(\tau_d\, v + D_{\min}\big)}, \qquad x = \big[D,\ v,\ v_L\big]^\top. \tag{9}$$

The chosen constants[1] are listed in Table 3.

Table 3. CBF parameters

Parameter	Symbol	Value
Safety time headway	τ_d	2 s
Minimum spacing	$D_{\min}$	6 m
Exponential–decay gain	γ_h	0.4

4.3. Safe set, boundary, interior

$$\mathcal{C} = \{x : h(x) \geq 0\}, \quad \partial\mathcal{C} = \{x : h(x) = 0\}, \quad \text{Int}\,\mathcal{C} = \{x : h(x) > 0\}.$$

$\mathcal{C}$ enforces the policy $D \geq \tau_d v + D_{\min}$; $\partial\mathcal{C}$ is the "safety wall"; Int $\mathcal{C}$ is strictly safe.

4.4. Extended class–$\mathcal{K}^\infty$ function

A map $\alpha : \mathbb{R} \to \mathbb{R}$ belongs to $\mathcal{K}^\infty$ when it is continuous, strictly increasing, $\alpha(0) = 0$, and unbounded as $r \to \pm\infty$. We adopt the linear choice

$$\boxed{\alpha(r) = \gamma_h\, r}, \qquad \gamma_h = 0.4 > 0, \tag{10}$$

which satisfies all criteria and yields exponential retreat from the boundary.

4.5. Gradient and Lie derivatives

$$\nabla_x h = [\,1,\ -\tau_d,\ 0\,], \qquad \|\nabla_x h\| = \sqrt{1+\tau_d^2} > 0.$$

With the longitudinal dynamics $\dot D = v_L - v,\ \dot v = u,\ \dot v_L = a_L$,

$$L_f h(x) = (v_L - v), \tag{11}$$

$$L_g h(x) = -\tau_d\ \ (< 0). \tag{12}$$

Since $L_g h(x) \neq 0$ everywhere, h depends affinely on u.

4.6. CBF inequality and safe–control set

Substituting $\alpha(r) = \gamma_h r$ into (8) gives the linear inequality

$$\boxed{(v_L - v)\ -\ \tau_d\, u\ +\ \gamma_h\, h(x)\ \geq\ 0.} \tag{13}$$

All inputs that satisfy (13) constitute

$$K_{\text{cbf}}(x) = \big\{u \in \mathbb{R} : (v_L - v) - \tau_d u + \gamma_h h(x) \geq 0\big\},$$

which is non-empty for every x because $L_g h = -\tau_d \neq 0$.

4.7. Forward invariance (Nagumo)

- **Interior** ($h > 0$)**:** If $u(x) \in K_{\text{cbf}}(x)$, $\dot h \geq -\gamma_h h$, so $h(t)$ decays at worst exponentially and never crosses zero.
- **Boundary** ($h = 0$)**:** Inequality (13) reduces to $v_L - v - \tau_d u \geq 0$. Because $L_g h$ is negative, there is always a suitable brake command, giving $\dot h \geq 0$.

Hence, by Nagumo's theorem, the headway set $\mathcal{C}$ is forward-invariant for any measurable feedback $u(x) \in K_{\text{cbf}}(x)$.

4.8. Summary

- Barrier map: $h = D - \tau_d v - D_{\min}$.
- Parameters: $\tau_d = 2\,\text{s},\ D_{\min} = 6\,\text{m},\ \gamma_h = 0.4$.
- $\nabla_x h \neq 0$ everywhere; $L_g h = -\tau_d \neq 0 \Rightarrow$ relative degree 1.

[1] τ_d is selected larger than the Lyapunov headway τ_{clf} to guarantee that safety dominates tracking.

- Linear extended $\mathcal{K}^\infty$ function ensures exponential (γ_h) decay toward the boundary.
- Inequality (13) defines a non-empty safe-control set K_{cbf}; Nagumo's condition proves forward invariance of $\mathcal{C}$.

5. Connected Cruise Controller (CCC)

5.1. Single-preceding-vehicle formulation

Connected Cruise Control augments ACC by incorporating cooperative speed tracking. The multi-vehicle law is here specialized to a pair *single* leader-follower.

5.2. Controller architecture

$$u_{\text{ref}} = A\big(V(D) - v\big) + B\big(W(v_L) - v\big), \tag{14}$$

where D is the gap, v the ego speed, v_L the lead speed, and $A, B > 0$ are proportional gains.

5.3. Range policy

$$V(D) = \max\Big\{0,\ \min\{\kappa(D - D_{\text{st}}),\ v\}\Big\}. \tag{15}$$

5.4. Speed policy

$$W(v_L) = \min\{v_L,\ v\}. \tag{16}$$

5.5. Combined behavior

The term $A[V(D) - v]$ restores progress, while $B[W(v_L) - v]$ damps relative speed, producing a spring-damper pair with stiffness $A\kappa$ and damping $A + B$.

Table 4. CCC parameters

Parameter	Symbol	Value
Range-error gain	A	0.5
Speed-error gain	B	0.5
Range-policy slope	κ	$0.2\,\text{s}^{-1}$
Stand-still gap	D_{st}	6 m

5.6. Role in the safety architecture

u_{ref} is forwarded to the CLF–CBF–QP layer; when no safety constraint is active the truck follows u_{ref} exactly, preserving comfort and cooperation.

6. Quadratic-Program (QP) Synthesis

6.1. Motivation

At each sampling instant we need an acceleration u that

(i) stays close to the nominal CCC command u_{ref},
(ii) satisfies the relaxed CLF inequality $L_f V + L_g V\, u \le -\varepsilon V + \delta$,
(iii) satisfies the CBF safety inequality $L_f h + L_g h\, u \ge -\gamma_h h$.

Because the CLF and CBF constraints are *affine* in (u, δ) and the comfort objective is quadratic, the problem is naturally posed as a *convex quadratic program*.

6.2. Decision vector

$$z = \begin{bmatrix} u \\ \delta \end{bmatrix} \in \mathbb{R}^2, \qquad \delta \ge 0 \text{ (CLF slack)}.$$

6.3. Cost functional

$$J(z) = \tfrac{1}{2}\,(u - u_{\text{ref}})^2 + \tfrac{1}{2}\,p\,\delta^2, \qquad p = 100 \gg 1. \tag{17}$$

Hessian matrix: Any quadratic can be written as

$$J(z) = \tfrac{1}{2}\, z^\top H z + f^\top z + c, \tag{18}$$

with

$$H = \begin{bmatrix} 1 & 0 \\ 0 & p \end{bmatrix}, \qquad f = \begin{bmatrix} -u_{\text{ref}} \\ 0 \end{bmatrix}, \qquad c = \tfrac{1}{2}\,u_{\text{ref}}^2.$$

$H \succ 0$ is diagonal, so the optimisation is strictly convex.

6.4. Affine inequality constraints

Origin	Inequality	Matrix row $a^\top z \le b$
CLF	$L_f V + L_g V\, u - \delta \le -\varepsilon V$	$a_1 = [L_g V, -1],\ b_1 = -L_f V - \varepsilon V$
CBF	$L_f h + L_g h\, u \ge -\gamma_h h$	$a_2 = [-L_g h, 0],\ b_2 = L_f h + \gamma_h h$
Slack	$\delta \ge 0$	$a_3 = [0, -1],\ b_3 = 0$
Input	$u_{\min} \le u \le u_{\max}$	$a_4 = [1, 0],\ b_4 = u_{\max}$; $a_5 = [-1, 0],\ b_5 = -u_{\min}$

6.5. QP statement

$$\begin{aligned} \min_{u,\delta}\ & \tfrac{1}{2}(u - u_{\text{ref}})^2 + \tfrac{1}{2}\,p\,\delta^2 \\ \text{s.t. } & L_f V + L_g V\, u - \delta \le -\varepsilon V, \\ & L_f h + L_g h\, u \ge -\gamma_h h, \\ & 0 \le \delta,\ u_{\min} \le u \le u_{\max}. \end{aligned} \tag{QP}$$

6.6. Feasibility logic

The CBF row is never relaxed; feasibility is guaranteed because $L_g h = -\tau_d \ne 0$ implies the constraint is always satisfiable. If CLF and CBF conflict, the optimiser increases δ, sacrificing convergence before safety. With $p = 100$ the slack remains small.

6.7. Convexity and solver

Diagonal H with positive entries and linear constraints ⇒ strictly convex problem with a unique global minimiser. QP solver: MATLAB's `quadprog`

Table 5. QP parameters

Parameter	Symbol	Value
Slack weight	p	100
Max propulsion	$u_{\max}$	$+2.75\,\text{m s}^{-2}$
Max braking	$u_{\min}$	$-5.5\,\text{m s}^{-2}$

6.8. Validation summary

- Convex: diagonal positive Hessian, affine constraints.
- Priority hierarchy: CBF hard, CLF soft (via δ), comfort softer.
- Forward invariance: CBF inequality unrelaxed ⇒ headway set remains safe.
- Stability: when CBF inactive ($h > 0$) slack is driven to zero, so the CLF inequality enforces exponential decay of V.

7. Lead-Vehicle Test Profiles

7.1. Table

Table 6. Acceleration scripts used to evaluate the safety-critical ACC.

No.	Scenario	Lead acceleration $a_L(t)$	Test objective
1	Cruise with mild oscillations	*Phase 1 (ramp-up):* $a_L = +3\,\mathrm{m\,s^{-2}}$ until $v_L \geq 25\,\mathrm{m\,s^{-1}}$. *Phase 2:* $a_L = 0.5\sin\big(2\pi{\cdot}0.2\,(t-t_0)\big)\,\mathrm{m\,s^{-2}}$.	Ride comfort and stability under gentle speed perturbations.
2	Single hard brake	*Phase 1:* same ramp-up as Profile 1. *Phase 2:* $a_L = 0$ for 10 s. *Phase 3:* emergency stop $a_L = -6.5\,\mathrm{m\,s^{-2}}$ to v_L=0. *Phase 4:* $a_L = 0$ thereafter.	Collision-avoidance performance during an isolated severe braking maneuver.
3	Noisy cruise transient	*Phase 1:* ramp-up as above. *Phase 2:* proportional hold $a_L = 0.2\,(25 - v_L)$. Measurement noise injected: $\sigma_D = 0.09$ m, $\sigma_v = 0.10\,\mathrm{m\,s^{-1}}$, $\sigma_a = 0.05\,\mathrm{m\,s^{-2}}$.	Robustness to sensor noise during benign steady cruising.

7.2. Output Plots

Here are the Plots for three different scenarios/profile.

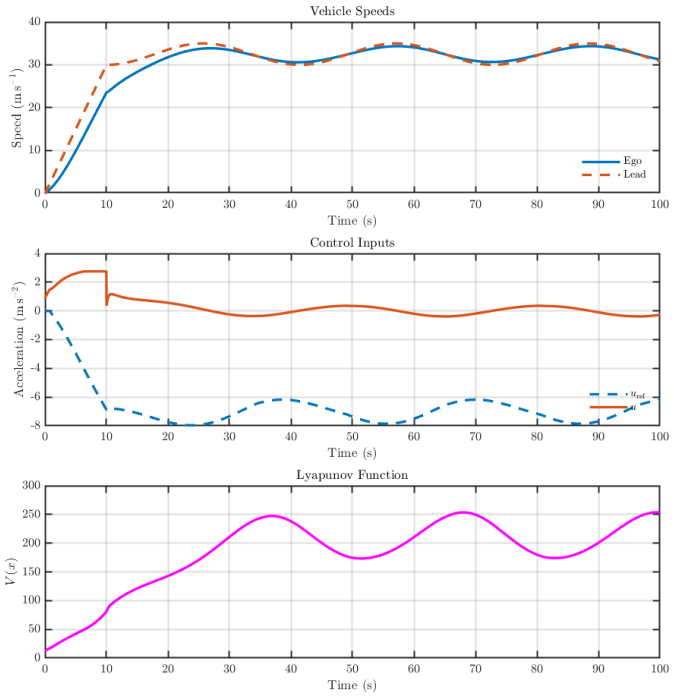

Figure 1. Scenario 1 part A

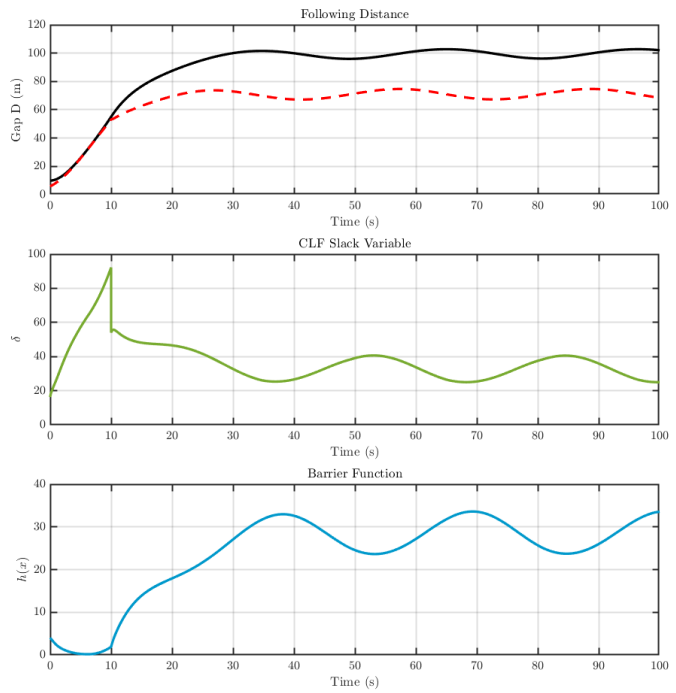

Figure 2. Scenario 1 part B

Observations:

Observations for Scenario 1:

- **Speed tracking:** The ego-truck speed (solid blue) closely follows the lead-car speed (dashed red) and its gentle 0.2 Hz oscillations around 33 m/s. An initial lag during ramp-up (0–20 s) settles into in-phase cruising thereafter.
- **Gap maintenance:** The following distance $D(t)$ increases from the start-gap (10 m) to about 95–100 m, oscillating synchronously with the speed fluctuations. No headway violations occur, as the barrier $h(x)$ remains positive.
- **Control inputs:** The nominal CCC command u_{ref} (blue dashed) exhibits ± 6 m/s^2 swings, whereas the filtered command u (orange solid) is much smoother (± 1 m/s^2), indicating minimal safety interventions under mild oscillations.
- **CLF slack δ:** Slack peaks near 90 during the start-up transient (around 15 s) when rapid gap closure conflicts with the CLF decrease. In steady cruising, δ settles to 25–40, showing only necessary stability relaxations.
- **Lyapunov function $V(x)$:** V rises to 250 during the transient and then oscillates mildly without unbounded growth, demonstrating effective enforcement of the CLF decrease condition.
- **Barrier function $h(x)$:** h quickly grows to 35 m and undulates gently with the speed waves. It remains strictly positive at all times, confirming forward invariance of the safety set.

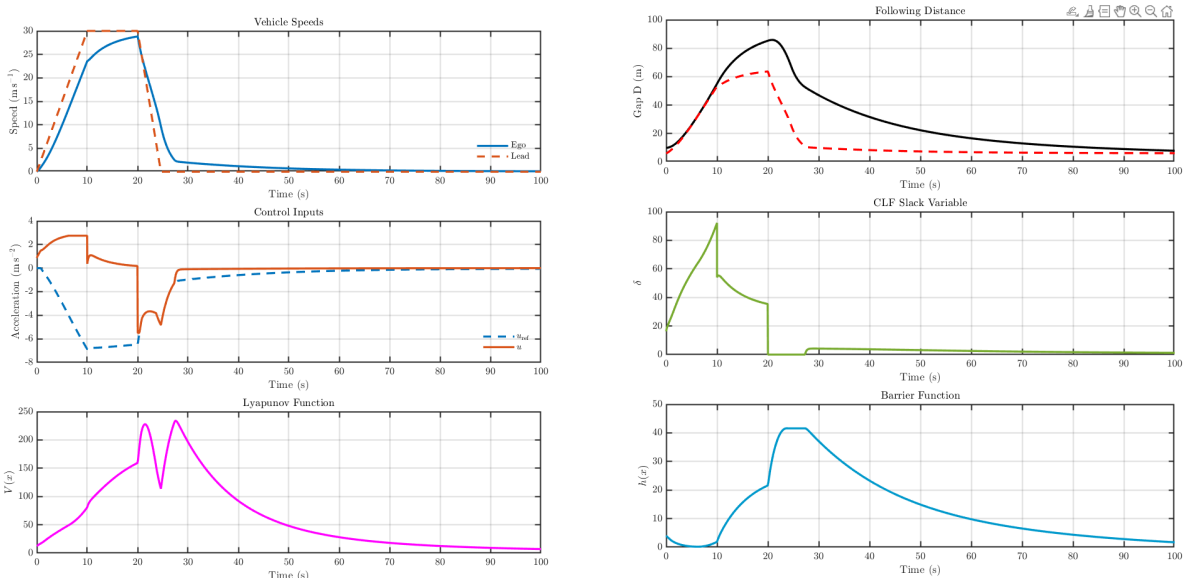

(a) Scenario 2 part A.

(b) Scenario 2 part B

Figure 3. Output Plots for Scenario 2

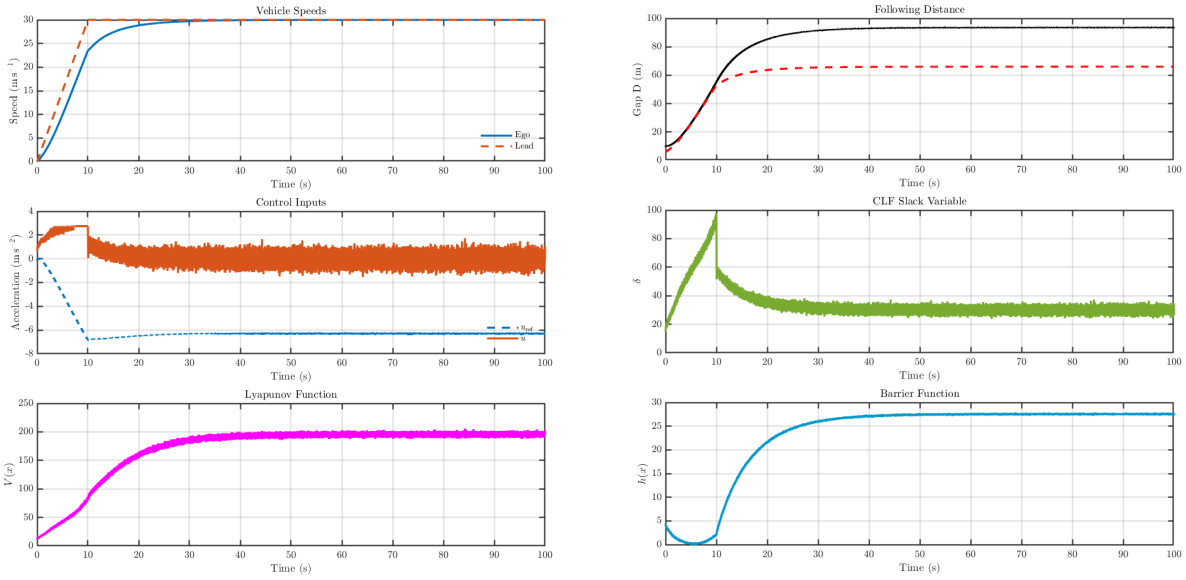

(a) Scenario 3 part A.

(b) Scenario 3 part B

Figure 4. Output Plots for Scenario 3

Observations for Scenario 2:

- **Speed response and delay:** The ego-truck accelerates nearly in lock-step with the lead vehicle up to the cruise speed (25 m/s). Upon the abrupt braking at 30 s, the truck's deceleration lags by about 1–2 s due to the QP capping at its maximum service-brake limit (−5.5 m/s²), illustrating the trade-off between safety enforcement and physical actuation bounds.
- **Gap collapse and recovery:** The following distance $D(t)$, which had grown to roughly 85 m, shrinks rapidly to 20 m during the hard brake, then increases slowly as the lead remains stopped. The slope of the gap recovery reflects the nominal CCC's minimal braking before coasting, ensuring the truck does not aggressively re-close the distance once the lead is halted.
- **Nominal vs. filtered input:**The nominal command u_{ref} plunges to −7 m/s² at the braking onset, but the actual acceleration u is constrained to −5.5 m/s² and exhibits a smoothed triangular profile as the QP trades off CLF convergence slack against safety. This demonstrates the QP's ability to moderate overly aggressive references while still guaranteeing barrier satisfaction.
- **Slack variable dynamics:**The slack $\delta(t)$ peaks sharply at 92 exactly when the lead's deceleration rate exceeds the truck's braking capability, temporarily relaxing the CLF condition. Once u saturates and the safety envelope is no longer threatened, δ falls dramatically to near zero by 35 s, indicating restoration of full CLF enforcement.
- **Lyapunov function behavior:**The Lyapunov measure $V(x)$ surges to 230 during the brake, capturing large speed and spacing errors. After the lead stops, V decays nearly exponentially, confirming that with slack relaxed only briefly, the system returns smoothly toward the desired equilibrium manifold.
- **Barrier function maintenance:**The barrier $h(x)$ jumps to approximately 40 m at brake onset—demonstrating a built-in safety margin above zero—and then decays gently toward zero without crossing it. The positive $h(t)$ throughout confirms forward-invariance: the truck never breaches the minimum headway despite extreme lead maneuvers.

Observations for Scenario 3:

- **Speed tracking under noise:** Although the ego truck converges to the lead's speed, small high-frequency oscillations ($\pm$0.2 m/s) persist, indicating that measurement noise is leaking into the control loop. A state estimator or low-pass filter could improve smoothness.
- **Gap steadiness—and jitter:** The gap $D(t)$ settles near 90 m but exhibits $\pm$0.5 m fluctuations. In safety-critical contexts, even sub-meter jitter can be undesirable; a smoother distance profile would enhance both comfort and perceived safety.
- **Control input volatility:** The filtered command u shows continuous small-amplitude noise ($\pm$0.5 m/s²). While within actuator limits, this chatter could excite mechanical resonances or increase wear. Penalizing $\dot{u}$ in the QP or using robust filtering could mitigate the effect.
- **Persistently high slack δ:** After the transient, δ remains around 30–35 instead of decaying toward zero. This indicates the CLF constraint stays substantially relaxed even when safety is assured, slowing convergence unnecessarily in noisy conditions.
- **Lyapunov function ripple:** $V(x)$ stabilizes near 200 but exhibits small ripples ($\pm$5), showing the system never attains true quasi-steady-state. This may impact energy efficiency and reduce control authority.
- **Barrier function noise sensitivity:** The safety margin $h(x)$ stays positive, but high-frequency dips (< 0.2 m) are visible. Although not unsafe, these dips could trigger spurious interventions; introducing a dead-band or a robust CBF formulation could avoid nuisance activations.

8. Conclusion

In this project we developed and validated a foundational safety-critical Adaptive Cruise Control (ACC) framework for a heavy-duty truck, built on Control Lyapunov Functions (CLFs), Control Barrier Functions (CBFs) and a real-time Quadratic Program (QP) filter. Rather than chasing full optimality from the outset, our goal was to construct a transparent, theoretically rigorous baseline that *always* puts safety ahead of aggressive performance.

Simulation across three representative lead-vehicle scenarios confirmed that the controller preserves safe headways, enforces Lyapunov stability, and respects realistic actuation limits—even during emergency braking and under noisy measurements. The noise-injected profile, however, exposed limitations in robustness: persistent input jitter, sustained CLF slack, and sensitivity to high-frequency disturbances. These observations point to clear opportunities for future enhancement.

The unavoidable tension between a desire for optimal performance and the uncompromising need for safety lies at the heart of modern autonomous systems. Our CLF–CBF–QP architecture addresses this tension directly by encoding both stability and safety in a mathematically verifiable way. Given the rising demand for high-performance *and* provably safe autonomy, we expect CLF–CBF frameworks to become staples in modern control engineering.

While the present controller is intentionally basic, it provides a robust platform for further work. Next steps include noise-aware state estimation, rate-penalised QP formulations, and adaptive barrier tuning—extensions that promise greater robustness without sacrificing the guarantees we have established.

On a personal note, this collaborative effort has reinforced for us the value of clarity, simplicity and principled theory in the pursuit of safe and reliable automated systems. We view the work reported here as a solid foundation on which deeper and more sophisticated control designs can be constructed.

References

[1] A. Alan, A. J. Taylor, C. R. He, A. D. Ames, and G. Orosz, "Control Barrier Functions and Input-to-State Safety With Application to Automated Vehicles," *IEEE Trans. Control Syst. Technol.*, vol. 31, no. 6, pp. 2744–2760, 2023.

[2] A. J. Taylor, A. Singletary, Y. Yue, and A. D. Ames, "Learning for Safety-Critical Control with Control Barrier Functions," in *Proc. NeurIPS Workshop on Safety-Critical Machine Learning*, PMLR, 2020, pp. 1–11.

[3] Y. Chen, G. Orosz, and T. G. Molnar, "Safe and Stable Connected Cruise Control for Connected Automated Vehicles with Response Lag," *arXiv:2409.06884*, 2024.

[4] S. Öncü, J. Ploeg, N. van de Wouw, and H. Nijmeijer, "Cooperative Adaptive Cruise Control: Network-Aware Analysis of String Stability," *IEEE Trans. Intell. Transp. Syst.*, vol. 15, no. 4, pp. 1527–1537, 2014.

[5] A. G. Ulsoy, H. Peng, and M. Çakmakcı, *Automotive Control Systems*. Cambridge Univ. Press, 2012.

[6] H. K. Khalil, *Nonlinear Systems*, 3rd ed. Upper Saddle River, NJ: Prentice Hall, 2002.

[7] Navistar International Corp., *International® ProStar® Day Cab Specification Card (TAD11036)*, Mar. 2016.

[8] Federal Highway Administration, *Statistics and Facts on U.S. Roadways*. Washington, DC: FHWA, 2023.